Journal of Pathology, Microbiology and Immunology

PMI
PATHOLOGY
MICROBIOLOGY
IMMUNOLOGY

ORIGINAL ARTICLE OPEN ACCESS

PMI Focus Issue 2026 – Artificial Intelligence in Diagnostic, Clinical and Forensic Pathology

Quantitative Histological Insights Into Sudden Arrhythmic Death Syndrome: Findings From a Forensic Autopsy Cohort

Pernille Heimdal Holm[1,2] | Thomas Hartvig Lindkær Jensen[3] | Joseph Westaby[4] | Mary Sheppard[4] | Stine Bøttcher Jacobsen[2,5] | Mikkel Eriksen Dupont[2,5] | Jeppe Dyrberg Andersen[5] | Bo Gregers Winkel[2] | Jacob Tfelt-Hansen[2,5] | Jytte Banner[1] | Kristine Boisen Olsen[1]

[1]Section of Forensic Pathology, Department of Forensic Medicine, Faculty of Health and Medical Sciences, University of Copenhagen, Copenhagen, Denmark | [2]Department of Cardiology, The Heart Centre, Copenhagen University Hospital, Rigshospitalet, Copenhagen, Denmark | [3]Department of Pathology, Copenhagen University Hospital, Rigshospitalet, Copenhagen, Denmark | [4]CRY Cardiovascular Pathology Unit, Cardiovascular Clinical Academic Group, Cardiovascular and Genetic Research Institute, City St George's University of London, London, UK | [5]Section of Forensic Genetics, Department of Forensic Medicine, Faculty of Health and Medical Sciences, University of Copenhagen, Copenhagen, Denmark

Correspondence: Pernille Heimdal Holm (heimdal@sund.ku.dk)

Received: 14 November 2025 | **Revised:** 2 February 2026 | **Accepted:** 6 February 2026

Keywords: artificial intelligence (AI) | cardiac morphology | postmortem | sudden arrhythmic death syndrome (SADS) | sudden cardiac death (SCD)

ABSTRACT

Sudden arrhythmic death syndrome (SADS) is a major cause of sudden cardiac death in young individuals, characterized by structurally normal hearts and negative toxicology. Although guidelines recommend family screening, phenotyping remains challenging. This study applied quantitative histology and deep-learning-based cell segmentation to investigate morphological features in SADS compared to controls. We conducted a retrospective autopsy study of 77 SADS cases and 41 age- and sex-matched controls (aged 1–49 years) who died from trauma or suicide. Cardiac tissue was analyzed using QuPath and deep learning-based image processing (Quan10). Random Forest classification and recursive feature elimination were used to identify discriminating features. Quantitative analysis found subtle but significant morphological differences. SADS cases had reduced residual myocardium in overall tissue (53% vs. 56%, $p = 0.02$) and endocardial regions (49% vs. 54%, $p < 0.001$). Endocardial and epicardial adipocyte density were key discriminators in the model. Genetic analysis identified pathogenic variants in six cases and three controls. AI-driven histology detected differences in hearts previously considered normal, suggesting subgroups within SADS. These findings support the use of quantitative tools in postmortem phenotyping, with potential to refine diagnosis, guide family screening, and improve understanding of arrhythmic mechanisms.

1 | Introduction

Sudden cardiac death (SCD) can be the first sign of a cardiac disease [1]. Autopsy is essential to determine the cause of death and identify inherited conditions that can guide genetic testing and family investigations [2–5]. In the forensic autopsy setting, SCD is defined as an unexpected sudden death due to either a cardiac or an unknown cause [3]. However, in many cases, the heart appears morphologically normal. These cases are labeled as sudden arrhythmic death syndrome (SADS), defined as sudden unexplained death in individuals older than 1 year with a morphologically normal heart or only minimal structural changes, no other pathological findings, and non-lethal toxicology [2, 3, 6]. SADS is a diagnosis of exclusion and accounts for over half of autopsied SCD

Abbreviations: CCI, Charlson Comorbidity Index; EAT, epicardial adipose tissue; HE, hematoxylin–eosin; LV, left ventricle; PSR, picrosirius red; RF, random forest; RFE, recursive feature elimination; RV, right ventricle; RVOT, right ventricular outflow tract; SADS, sudden arrhythmic death syndrome; SCD, sudden cardiac death.

under 35 years in Denmark [7, 8] with reported prevalence ranging from 4% to 53% internationally [9–13].

Current guidelines recommend referral of all SADS cases to specialist cardiologists for evaluation [3]. However, the absence of structural abnormalities complicates the diagnosis, and existing postmortem tools are limited. Autopsy-based cardiac phenotyping combines circumstances of death, medical history, toxicology, and a systematic cardiac examination to distinguish morphologically normal hearts (SADS) from structural abnormalities [2, 5]. SADS has been associated with cardiac channelopathies (e.g., long QT syndrome and Brugada syndrome) [14, 15] and with concealed cardiomyopathies, in which arrhythmogenic variants may exist despite minimal or absent structural changes [16, 17]. Subtle fibrosis in the right ventricular outflow tract has been suggested as a potential arrhythmic substrate in Brugada syndrome (BrS) [18, 19].

Histopathological evaluations of SADS remain challenging, as subtle findings often have unclear significance [20–22]. Conventional microscopy is qualitative and may miss subtle features, and few studies have applied systematic, quantitative analyses to postmortem cardiac tissue. To address this gap, we applied quantitative histology and deep learning-based cell segmentation to identify histological and cellular features of SADS cases compared with age- and sex-matched controls. The aim was to identify subtle morphological differences that may characterize subgroups within SADS.

2 | Materials and Methods

This retrospective autopsy study was conducted at the Department of Forensic Medicine, University of Copenhagen, Denmark. The study population comprised SCD victims autopsied at the department between 2009 and 2011. The selection criteria are illustrated in Figure 1, and included cases with ages between 1 and 49 years, natural or unknown manner of death, and cardiovascular or unknown cause of death. Subjects were excluded if the cause of death was ischemic heart disease, cardiomyopathy, congenital heart disease, valve disease, or non-cardiac (e.g., pulmonary embolism, brain aneurysm, or aortic dissection). Similarly, an age- and sex-matched control group was selected from the years 2006–2011 with individuals aged 1–49 years whose manner of death was either accidental or suicide with no cardiac disease or drug overdose.

2.1 | Autopsy and Tissue Collection

All cases were autopsied according to accredited departmental procedures (ISO 17020). Cardiac examinations were performed

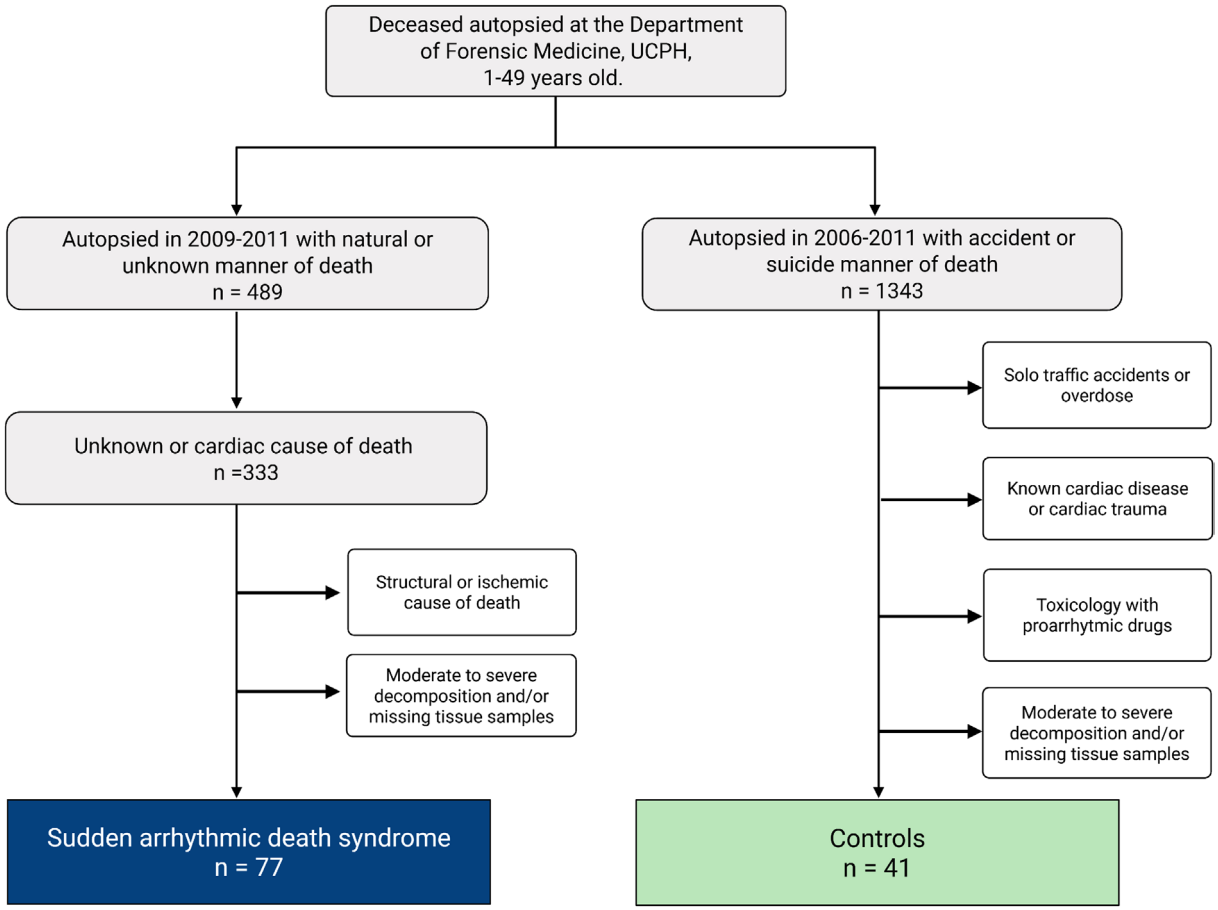

FIGURE 1 | Flowchart illustrating the study population, including inclusion and exclusion criteria applied during case selection. The diagram outlines the process from initial autopsy to final inclusion of SADS cases and controls, conducted at the Department of Forensic Medicine, University of Copenhagen (UCPH). Created with Biorender.com. Holm, P. (n.d.) https://BioRender.com/q0p34cd.

according to the AECVP guidelines [5]. At autopsy, at least four transmural cardiac samples were collected from the midventricular slice: anterior and posterior left ventricle (LV), right ventricle (RV), and septum. Additional samples from LV and RV were obtained only when cardiac disease was suspected and were solely used for re-evaluation of cardiac diagnosis during SADS case selection. Right ventricular outflow tract (RVOT) samples were not routinely collected at the time and are not included in this study. All underwent histological examination. Toxicology was negative in all cases.

From the autopsy report, the information provided by the police included the circumstances of death (witnessed or unwitnessed), activity before death, and possible comorbidities reported by general practitioners or relatives. Comorbidities were categorized using the Charlson Comorbidity Index (CCI) score [23].

2.2 | Tissue Preparation

Four standard midventricular tissue samples (RV, anterior LV, posterior LV, septum) were fixed in formalin, embedded in paraffin (FFPE), and 3 μm sections were cut and stained with hematoxylin–eosin (HE) and picrosirius red (PSR). All samples were whole slide scanned using a Hamamatsu S60 NanoZoomer (Hamamatsu Corp., Hamamatsu, Shizuoka, Japan). The four samples were scanned at a x20 resolution for both HE and PSR staining. Additionally, three HE-stained samples (RV, anterior LV, and septum) were scanned at x40 resolution.

2.3 | Re-Evaluation of the Original Diagnosis

All cases of SCD were re-evaluated by an expert panel after excluding cases with decomposition. Each case was microscopically re-examined to ensure that it met the criteria for SADS [12, 24]. Detailed information about the re-evaluation process is available in the Supporting Information S1.

2.4 | Genetics

Genetic data were available for 73 of the 77 SADS cases and 16 of 41 controls. DNA was extracted from frozen blood ($n = 71$), frozen muscle ($n = 1$), FFPE muscle ($n = 7$), FFPE spleen ($n = 1$), or FFPE kidney ($n = 9$) using the QIAamp DNA Blood Mini kit (Qiagen, Germany), QIAamp DNA Mini Kit (Qiagen, Germany), or QIAamp DNA FFPE Tissue Kit (Qiagen, Germany).

For 32 of 73 SADS cases, which were included and described in previous studies [25, 26], the coding regions of 100 genes were sequenced using a custom design of the HaloPlex Target Enrichment system (Agilent Technologies, USA). For four SADS cases, whole exome sequencing (WES) was performed using the SureSelect^{XT} Target Enrichment System for Illumina with the SureSelect Clinical research Exome library (Agilent Technologies, USA). For the remaining 37 SADS cases, whole genome sequencing (WGS) was performed using the TruSeq DNA PCR-free kit (Illumina, USA) or the TruSeq DNA Nano kit (Illumina, USA). Sequencing was performed on Illumina platforms (MiSeq, NextSeq 500, or NovaSeq 6000) for all cases.

Bioinformatic processing of sequencing data was performed as previously described [25–27]. Briefly, adapter sequences and low-quality bases were removed, the sequencing reads were aligned to the human reference genome, and genetic variants were identified. Only single nucleotide variants with a read depth (DP) ≥ 8 and Genome Analysis Toolkit (GATK) Genotype Quality (GQ) ≥ 10 were included in subsequent analyses. Homozygous variant calls were defined as one allele being called in $> 80\%$ of the locus sequencing reads, whereas heterozygous variant calls were defined as two alleles having frequencies between 33.3% and 66.7% of the locus sequencing reads. To ensure comparability among all investigated individuals, only regions that were covered by all three sequencing approaches (100 gene panel, WES, and WGS) were investigated. Several genes included in the original 100 gene panel have limited evidence for association with inherited cardiac disease. To ensure analysis of genes with strong evidence for disease association, only genes on the "ACMG SF v3.2 list for reporting of secondary findings in clinical exome and genome sequencing" [28] were assessed. Hence, genetic variation in the following 29 genes were investigated: *ACTC1, BAG3, CALM1, CALM2, CALM3, CASQ2, DES, DSC2, DSG2, DSP, GLA, KCNH2, KCNQ1, LMNA, MYBPC3, MYH7, MYL2, MYL3, PKP2, PRKAG2, RBM20, RYR2, SCN5A, TMEM43, TNNC1, TNNI3, TNNT2, TPM1, TTN*. For variants in *TTN*, only frameshift and nonsense variants, as well as splice site variants located in exons with a percent spliced in (PSI) value $\geq 90\%$ were assessed [29]. The pathogenicity of genetic variants was assessed using the American College of Medical Genetics and Genomics (ACMG) guidelines [30]. To assess population frequencies, gnomAD v4.1.0 was used. All genetic variants are reported in GRCh38/hg38 coordinates.

2.5 | Digital Image Analysis Methods

2.5.1 | QuPath

Four standard PSR-stained samples were analyzed using QuPath software following the previously published pipeline [31]. Briefly, fibrosis and myocardial tissue were automatically quantified using a pixel classifier, and adipocytes were detected using the Cellpose algorithm. The method has been validated against manual assessment in the original publication. Regions were subdivided into endocardium, midmyocardium, epicardium, and epicardial adipose tissue (EAT). The resulting data were exported for further statistical analysis.

2.5.2 | Quan10—Machine Learning Based Image Processing

Three HE-stained samples (anterior left ventricle, right ventricle, and septum) were analyzed with Quan10 due to extensive data and time required for deep learning-based processing. Representative regions were selected to capture full wall representation while maintaining feasibility. These regions were processed by Quan10 for automated segmentation and classification of myocytes and other cellular features.

Inference-leveraging machine learning utilized a processing pipeline that included segmentation and subsequent

classification of cells. The deep learning convolutional neural network (CNN) model Hover-net from Graham et al. [32] was used for instance segmentation of cell nuclei and trained on Gamper et al. PanNuke dataset [33]. The classification process involved a CNN model that was influenced by the ResNet framework [34]. From each segmented cell, exhaustive morphological quantifications were registered, for example, granularity using gray-level co-occurrence matrices [35] and metrics derived from cell nuclei [36] collectively termed as morphological features.

For cell classification, an experienced cardiac pathologist (THLJ) used a dataset of approximately 70 FFPE HE-stained cardiac tissue samples from a previous cohort of COVID-19 deaths [37]. In total, 64×64 pixel patches of 1590 myocytes, 141 lymphocytes, 1516 mesenchymal cells, and 122 other cells were included as training data. A multiclass RESNET network was trained to identify cell classes. The performance metrics after 100 epochs of training had a validation accuracy of 94.4, an accuracy of 97.69, and a loss of 0.0729 (cross-entropy loss function). An example of the cellular segmentation is shown in Figure 2.

Cellular data from all samples were compressed into a single dataset in R (version 4.3.1) [38, 39]. Myocytes and lymphocytes were selected using a probability threshold of ≥80%. An extensive list of the measured morphological features is provided in the Supporting Information S2.

2.6 | Statistics

Statistical analyses were performed in R (version 4.3.1; R Foundation for Statistical Computing, Vienna, Austria) using RStudio [38, 39]. Means, medians, standard deviations, and interquartile ranges were calculated. Groups were compared using Wilcoxon rank-sum test for continuous variables and Pearson's chi-squared test or Fisher's exact test for categorical variables. A *P*-value ≤0.05 was considered statistically significant; no adjustment for multiple comparisons was made due to the exploratory nature of the study.

The large cellular and histological dataset was normalized for comparison. Random forest (RF) classification was conducted using the *randomForest* package (version 4.7.1.1) [40], initially including all features. Training and test sets were split 70/30, and the training set was balanced using Random Over-Sampling Examples (*ROSE*, version 0.0.4) [41]. Features with a mean decrease in Gini >0.95 were included in subsequent subset analysis. Model performance was evaluated using confusion matrix, standard metrics, and receiver operating characteristic (ROC) curves with area under the curve (AUC) values. Recursive feature elimination (RFE) using the *caret* package (version 6.0.94) [42] was applied as an alternative method to identify features distinguishing cases and controls.

Additional R Packages used for data management, visualization, and performance metrics were *PRROC* (version 1.3.1) [43], *pROC* (version 1.18.5) [44], *GGally* (version 2.2.1) [45], *tidyverse* (version 2.0.0) [46], *readxl* (version 1.4.3) [47], *flextable* (version 0.9.6) [48] and *gtsummary* (version 1.7.2) [49].

2.7 | Ethics Statement

The study was approved by the National Committee on Health Research Ethics, Denmark (H-19084051 and H-2-2012-017), and by the Faculty of Health and Medical Sciences, University of

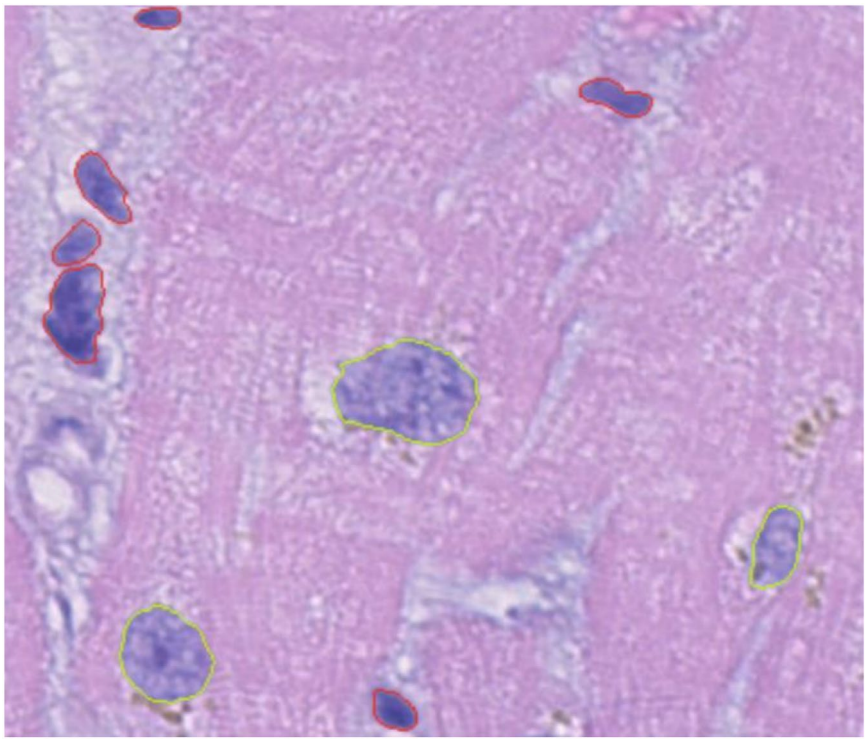

FIGURE 2 | Example of the Quan10 algorithm with cellular segmentation and classification in HE-stained cardiac samples. Red outlines indicate endothelial cells, and green outlines indicate cardiomyocyte nuclei.

Copenhagen (514–0671/21–3000 and 514–0725/22–3000). The study adhered to the principles of the Declaration of Helsinki. The Danish Law stipulates that consent from the next of kin is not required in cases before 2012 and was therefore not obtained in this study. A collaboration agreement was obtained between the Department of Forensic Medicine, Faculty of Health and Medical Sciences, University of Copenhagen, and CRY, Cardiovascular Pathology Unit, City St. George's University of London, London, United Kingdom (MTA2024-145).

3 | Results

After re-evaluation of the original diagnoses, the study included 77 SADS cases and 41 age- and sex-matched controls. The cohorts were generally comparable (Table 1). Statistically significant differences were observed for the proportion of witnessed deaths (21% vs. 63%, $p<0.001$), activity at death, and prevalence of psychiatric diseases, which was higher in SADS cases (30% vs. 7.3%, $p=0.005$). Substance abuse trended higher in SADS cases (25% vs. 9.8%, $p=0.051$). Heart weight and LV wall thickness did not differ significantly between groups. Genetic analysis identified likely pathogenic (LP) variants in six SADS cases (*PKP2, RBM20, TTN (two cases), SCN5A, and DSP*) and in three control cases (*TTN* only). No pathogenic variants were detected. Full details are provided in the Supporting Information S3.

Quantitative QuPath analysis revealed lower myocardial percentages in SADS cases compared to controls: total tissue combined (53% vs. 56%, $p=0.02$), endocardial region (49% vs. 54%, $p<0.001$), septum (55% vs. 61%, $p=0.007$), and RV (40% vs. 47%, $p=0.002$) (Table 2). These differences are illustrated in the violin plots in Figure 3, which shows a tail-like distribution in SADS cases, whereas control cases showed a more uniform distribution.

An RF classification model was employed to evaluate the relative importance of histological and cellular features in

TABLE 1 | Characteristics of the overall study population, SADS group, and control group with comparisons.

Characteristics	Overall ($N=118$)	SADS ($n=77$)	Controls ($n=41$)	p-value
Age at death (years)	38 (29–43)	38 (29–43)	39 (28–43)	0.80
Sex (male)	84 (71%)	55 (71%)	29 (71%)	>0.90
Witnessed	42 (36%)	16 (21%)	26 (63%)	**<0.001***
Activity at death				
Rest	15 (13%)	14 (18%)	1 (2.4%)	**0.015***
Daily activity	27 (23%)	12 (16%)	15 (37%)	**0.010***
Physical activity	7 (5.9%)	6 (7.8%)	1 (2.4%)	0.40
Unknown	69 (58%)	45 (58%)	24 (59%)	>0.90
Resuscitation	52 (44%)	37 (48%)	15 (37%)	0.20
Comorbidities				
Hypertension	7 (5.9%)	6 (7.8%)	1 (2.4%)	0.40
Hypercholesterolemia	1 (0.8%)	1 (1.3%)	0 (0%)	>0.90
Psychiatric disease	26 (22%)	23 (30%)	3 (7.3%)	**0.005***
Substance abuse	23 (19%)	19 (25%)	4 (9.8%)	0.051
CCI score				
0	106 (90%)	66 (86%)	40 (98%)	0.055
1	9 (7.6%)	8 (10%)	1 (2.4%)	0.20
2+	3 (2.5%)	3 (3.9%)	0 (0%)	0.60
Autopsy findings				
BMI (kg/m^2)	25 (22–29)	25 (23–30)	24 (21–28)	0.15
Heart weight (g)	368 (316–409)	374 (330–418)	364 (295–402)	0.09
LV wall (mm)	14 (12–15)	14 (13–15)	13 (12–15)	0.07
RV wall (mm)	4 (3–4)	4 (3–4)	4 (3–4)	0.80

Note: Values are presented as n (%) or medians (Q1–Q3). The CCI scores were based on information from police reports. Statistical analyses were performed using the Wilcoxon rank-sum test, Pearson's chi-squared test, and Fisher's exact test.
Abbreviations: BMI, Body mass index; CCI, Charlson Comorbidity Index; LV, left ventricle; RV, right ventricle; SADS, Sudden arrhythmic death syndrome.
*Statistically significant values ($p\leq0.05$) are indicated in bold.

TABLE 2 | QuPath results in the overall study population with a comparison between SADS and controls.

	Overall ($N=118$)	SADS ($n=77$)	Controls ($n=41$)	p-value
Total tissue (without epicardial adipose tissue)				
Myocardium (%)	54 (49–60)	53 (46–59)	56 (52–60)	**0.02***
Fibrosis (%)	28 (22–33)	29 (23–37)	26 (21–32)	0.15
Adipocytes (per mm^2)	5 (3–9)	5 (3–10)	5 (3–8)	0.09
Epicardial region				
Myocardium (%)	55 (44–60)	53 (43–60)	55 (49–62)	0.08
Fibrosis (%)	27 (22–35)	27 (22–37)	26 (20–31)	0.20
Adipocytes (per mm^2)	11 (6–20)	12 (6–23)	9 (4–18)	0.08
Mid region				
Myocardium (%)	61 (53–67)	59 (52–66)	62 (55–67)	0.14
Fibrosis (%)	25 (20–30)	25 (21–31)	24 (19–28)	0.20
Adipocytes (per mm^2)	4 (2–7)	4 (2–8)	3 (2–6)	0.20
Endocardial region				
Myocardium (%)	51 (46–56)	49 (42–54)	54 (49–59)	**<0.001***
Fibrosis (%)	30 (24–37)	31 (25–39)	28 (22–35)	0.08
Adipocytes (per mm^2)	2 (1–4)	2 (1–5)	2 (1–3)	0.09
Left ventricle				
Myocardium (%)	56 (49–62)	56 (48–61)	57 (51–64)	0.09
Fibrosis (%)	26 (21–32)	27 (21–35)	24 (20–30)	0.09
Adipocytes (per mm^2)	3 (2–4)	3 (2–4)	2 (1–4)	0.20
Septum ($n=115$)				
Myocardium (%)	58 (50–62)	55 (48–61)	61 (55–64)	**0.007***
Fibrosis (%)	28 (22–34)	29 (23–37)	26 (19–31)	0.09
Adipocytes (per mm^2)	1 (0–2)	1 (1–3)	1 (0–2)	0.10
Right ventricle ($n=113$)				
Myocardium (%)	42 (35–50)	40 (32–50)	47 (41–52)	**0.002***
Fibrosis (%)	35 (28–41)	35 (28–41)	33 (30–41)	0.40
Adipocytes (per mm^2)	23 (11–41)	24 (13–47)	20 (7–34)	0.06

Note: Data from the epicardial, mid-, and endocardial regions were compiled across the ventricles, and for septum from the endocardial and midregion. Total tissue included all sample and regions averaged excluding the epicardial adipose tissue. Tissue samples were excluded from the right ventricle in five cases and the septum in three cases because of tangential or incorrect sampling. Values represent medians (Q1–Q3). Statistical analysis was performed using the Wilcoxon rank-sum test.
Abbreviation: SADS, sudden arrhythmic death syndrome.
*Statistically significant values ($p \leq 0.05$) are indicated in bold.

distinguishing SADS from controls. The model, as illustrated in Figure 4, achieved an AUC of 0.73, indicating moderate discrimination with accuracy, sensitivity (recall), and specificity of 72.4%, 66.7%, and 78.6%, respectively. Adipocyte density in the endocardial region was the most important variable (mean decrease in Gini ~4.8), followed by myocardial proportion in the endocardial region and epicardial regions, and epicardial adipocyte density (Supporting Information S4). At the cellular level, only two features (mean lymphocyte ferret diameter max and cardiomyocyte nucleus equivalent diameter area) were retained in the RF subset model.

RFE analysis identified additional features of potential importance. Approximately 10 features were optimal based on accuracy, and highly correlated features ($r>0.9$) were excluded (Supporting Information S5). Important features included those identified by the RF model as well as additional cellular characteristics, such as mean cardiomyocyte nucleus area, minimum

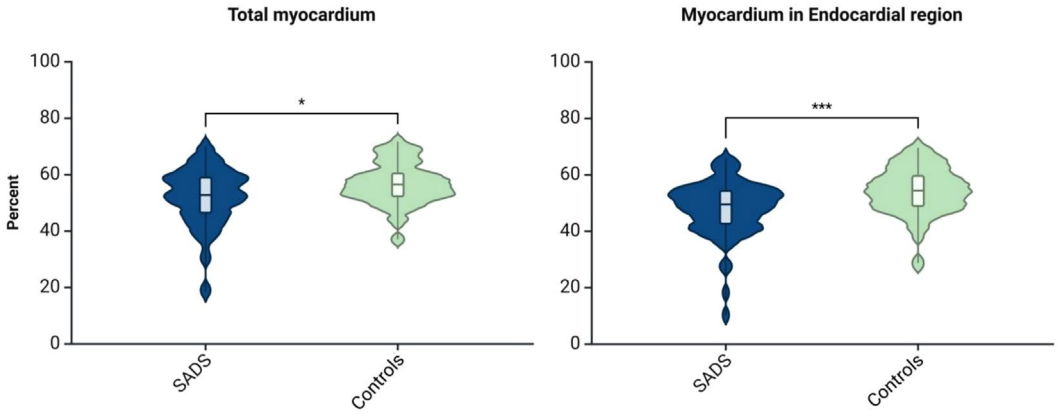

FIGURE 3 | Violin plots comparing the percentage of total myocardium and myocardium in the endocardial region between SADS and controls. SADS shows a statistically significant reduction in myocardium percentage and a wider distribution compared to controls. Statistical significance ($p \leq 0.05$) is indicated with asterisks (*). SADS, sudden arrhythmic death syndrome. Created with Biorender.com. Holm, P. (n.d.) https://BioRender.com/q0p34cd.

		Reference	
		SADS	Controls
Prediction	SADS	10	3
	Controls	5	11

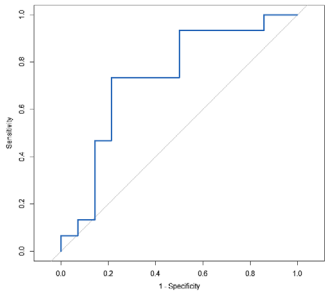

FIGURE 4 | Figure showing two panels. First panel displays a confusion matrix comparing predicted and true labels for SADS and controls using a random forest model. The second panel shows a ROC curve with an AUC of 0.73, illustrating the model's ability to differentiate between SADS and controls. SADS, sudden arrhythmic death syndrome; ROC, receiver operating characteristic; AUC, area under the curve.

intensity, intensity standard deviation, and nearest-neighbor distance.

4 | Discussion

This study identified subtle histological differences between SADS cases and non-cardiac controls, including reduced myocardial content and changes in adipocyte density, suggesting potential morphological subgroups within SADS.

We found a lower percentage of myocardial tissue in the endocardial region, particularly in the septum and RV, in SADS cases compared to controls. While fibrosis was not significantly different overall, epicardial fibrosis emerged as an important feature in the RF analysis. Both fibrosis and fat infiltration can constitute a substrate for reentry arrhythmia, potentially contributing to SADS pathophysiology [50–52]. Epicardial fibrosis is characteristic of arrhythmogenic cardiomyopathy (ACM) [21], whereas endocardial fibrosis is more typical of idiopathic forms [53]. The presence of epicardial fibrosis in SADS may therefore represent concealed ACM, suggesting early structural changes [22]. BrS and ACM may represent phenotypically different presentations within a shared disease spectrum [54]. BrS has been associated with fibrous replacement in the RVOT [18], which was not sampled in our cohort. Studies incorporating automated RVOT quantification and genetic examination are warranted to further elucidate disease pathogenesis. These findings also emphasize the role of the autopsy in SADS to enable accurate diagnosis, but declining autopsy rates remain a significant barrier underscoring the need for close collaboration between pathologists and cardiologists [55].

RF analysis also revealed adipocyte density in the endocardial region as a key discriminator between SADS and controls. Fatty infiltration in the RV is generally considered a normal phenomenon [21, 56–58]. However, computational models suggest that adipose tissue may trigger cardiac arrhythmias and serve as a substrate for reentry arrhythmia. Whether fibrosis poses a greater arrhythmic risk than fat infiltration remains unclear. Some studies indicate that fat has a lesser impact [59], while others propose that infiltrating adipose tissue could be more significant than a fibrotic scar in determining the arrhythmic burden and promoting ventricular arrhythmias [52]. The fibrosis and fatty infiltration observed in this study could also represent reactive changes secondary to arrhythmia, potentially driven by genetic variants affecting ion channel function [50, 51]. Advanced quantitative techniques could enable refined postmortem phenotyping of SADS, revealing subgroups based on fibrous versus fatty replacement. Fatty infiltration may increase with higher body mass index (BMI) and could represent a potential confounder when interpreting adipocyte density findings [58]. In the present study, BMI did not differ significantly between groups. Obesity is associated with cardiac hypertrophy, increased right ventricular epicardial fat, and left ventricular fibrosis [60]. The detected subtle changes could represent obesity-related changes; however, these findings require further validation.

Genetic analysis identified variants in genes associated with cardiomyopathies. Specifically, *PKP2* and *DSP*, both linked to ACM, were identified in two cases, whereas *RBM20*, predominantly associated with familial dilated cardiomyopathy, was found in one case [61, 62]. These individuals may represent cases

of concealed cardiomyopathy [16, 17]. This supports the notion that sudden death can occur at any point along the disease spectrum, including in the absence of overt structural abnormalities. Only one case had a variant in a channelopathy-associated gene (*SCN5A*), linked to BrS, long QT syndrome, and dilated cardiomyopathy [63]. Variants in *TTN* were observed in two SADS cases and three controls. Although *TTN* variants are associated with dilated cardiomyopathy, their clinical interpretation remains challenging due to bioinformatic limitations in assessing pathogenicity and their relatively high allele frequency in the general population (1%–3%) [29, 64–65]. Further studies are needed to explore the relationship between genotype and improved morphological phenotypes in SADS, and to better delineate subgroups with a high likelihood of inherited cardiac disease. Recent long-term follow-up data show that 12% of relatives of SCD victims are diagnosed with an inherited cardiac disease, highlighting the relatively low yield of family screening and underscoring the need for improved postmortem phenotyping to better target the high-risk families [66].

The characteristics of our SADS cohort broadly align with previous studies, being primarily male (71%) with a median age of 38 years [11, 24]. However, the circumstances of death differed: 58% were unwitnessed, 18% occurred during sleep or rest, and only 21% were witnessed, in contrast to prior reports [11]. Psychiatric disorders were more common in SADS cases than in controls, consistent with earlier studies [11, 67]. Although the mechanisms remain unclear, medication use, behavioral and lifestyle factors may contribute to arrhythmic vulnerability, as well as selection bias, since individuals with severe psychiatric disease are overrepresented in autopsy studies [68, 69]. To evaluate health status, we assessed comorbidities using police reports and information from relatives or general practitioners. The reliability of these data varies, particularly concerning substance abuse and psychiatric diseases [70]. Both conditions, also in conjunction, have been linked to SCD and cardiac changes [21, 69, 71–72]. The reliability of these data represents a limitation to this study and limits our possibility to examine the possible effects of chronic use of psychotropic drugs on the heart. Overall, most SADS cases appeared healthy: 86% had a CCI score of zero [23]. This aligns with previous reports and supports that SADS occurs in otherwise apparently healthy individuals [67]. Importantly, individuals with substance abuse or psychiatric disorders may represent distinct subgroups within SADS, with a lower likelihood of underlying inherited cardiac disease. Recognizing such cases has clinical value, as it may help reduce unnecessary concern among families regarding heritable cardiac risk. Future studies of SADS should incorporate systematic assessment of these conditions using reliable Danish registry data to explore the potential contribution to subtle myocardial pathology.

In this study, we used standard samples available for all cases to avoid introducing bias. Cardiac structural changes can be focal, and it cannot be ruled out that potential structural changes were not detected due to the limited sampling. All available samples were examined and deemed morphologically normal in both SADS and control cases. However, sampling did not include RVOT, which may be critical for detecting fibrous changes in arrhythmic disorders, such as BrS and concealed ACM [18, 73]. By using standardized samples across all cases, we ensured uniformity. Even with this limitation, our approach was able to detect significant differences in cardiac tissue between SADS cases and controls. All samples were FFPE after autopsy; however, some had suboptimal quality, requiring exclusion. In other cases, PSR staining was faint from tissue degradation, affecting the algorithm's ability to quantify myocardial tissue [31]. The violin plot showed extreme outliers with low myocardial percentages, particularly in the endocardial region. This could be due to the staining variability, or papillary muscle attachment sites within the endocardial regions, which could artificially elevate fibrosis measurements.

Key strengths include the large cohort size and matched control group, allowing meaningful comparisons of pathological findings. Some SADS cohorts included cases with cardiac morphological findings of unknown significance [22, 74]. Such cases were excluded after expert re-evaluation in our study. Thus, the study focused on SADS cases without detectable structural abnormalities at gross or histopathological levels. Research suggests that referral to expert cardiac pathologists increases the proportion of cases classified as SADS [75, 76]. Enhancing the characterization of SADS and identifying phenotypic subgroups may improve understanding of the underlying pathophysiology. A major advantage is the use of digital image analysis, which enables objective quantification of tissue morphology and cell features.

In this study, we applied quantitative histology to investigate morphological differences between SADS cases and controls, cases considered normal by conventional methods. Our findings showed a modest reduction in residual myocardium in SADS cases. RF analysis distinguished SADS cases from controls, identifying epicardial fibrosis and endocardial adipocyte density as key discriminative features.

These results suggest potential morphologically distinct subgroups within SADS. Further studies with larger, independent cohorts are needed to validate these findings. The identified features may contribute to more precise postmortem phenotyping of SADS, potentially aiding the classification of cases and identifying individuals less likely to have died from an inherited arrhythmic condition. Future studies should explore the integration of AI-based histological profiling into routine autopsy practice and workflows to enhance the diagnostic yield in sudden cardiac death cases and guide the targeted family screening and follow-up.

Acknowledgements

The authors wish to acknowledge the families of the deceased for their contribution to this research. We extend our sincere appreciation to our laboratory technicians at the Department of Forensic Medicine, UCPH, for their meticulous preparation and scanning of the histological samples. We acknowledge the Core Facility for Integrated Microscopy (CFIM), Faculty of Health and Medical Sciences, University of Copenhagen.

Funding

This study was funded by the Department of Forensic Medicine, Faculty of Health and Medical Sciences at the University of Copenhagen, Denmark. B.G.W. received funding from the Novo Nordisk Foundation,

Denmark (Grant NNF23OC0082432). J.T.H. received funding from the Novo Nordisk Foundation Distinguished Investigator Program (Grant 0088546). T.H.L.J. received funding from the BETA.HEALTH Innovation Platform (Grant 2022-1133) and is owner of the QUAN10 AI software. PHH received a travel grant from the Danish Cardiovascular Academy.

Conflicts of Interest

J.T.H.: Consulting Fees/Honoria Boston Scientific, Cytokinetics, Solid Bioscience. The other authors declare no conflicts of interest.

Data Availability Statement

Data is available from the Department of Forensic Medicine, UCPH, but access is restricted under the study licenses. This data is not publicly available.

References

1. T. H. Lynge, B. Risgaard, R. Jabbari, et al., "Cardiac Symptoms Before Sudden Cardiac Death Caused by Hypertrophic Cardiomyopathy: A Nationwide Study Among the Young in Denmark," *Europace* 18 (2016): 1801–1808.

2. M. K. Stiles, A. A. M. Wilde, D. J. Abrams, et al., "2020 APHRS/HRS Expert Consensus Statement on the Investigation of Decedents With Sudden Unexplained Death and Patients With Sudden Cardiac Arrest, and of Their Families," *Heart Rhythm* 18 (2021): 1–50.

3. K. Zeppenfeld, J. Tfelt-Hansen, M. de Riva, et al., "2022 ESC Guidelines for the Management of Patients With Ventricular Arrhythmias and the Prevention of Sudden Cardiac Death," *European Heart Journal* 43 (2022): 3997–4126.

4. S. L. Harris and S. A. Lubitz, "Clinical and Genetic Evaluation After Sudden Cardiac Arrest," *Journal of Cardiovascular Electrophysiology* 31 (2020): 570–578.

5. C. Basso, B. Aguilera, J. Banner, et al., "Guidelines for Autopsy Investigation of Sudden Cardiac Death: 2017 Update From the Association for European Cardiovascular Pathology," *Virchows Archiv* 471 (2017): 691–705.

6. T. Tsuda, K. K. Fitzgerald, and J. Temple, "Sudden Cardiac Death in Children and Young Adults Without Structural Heart Disease: A Comprehensive Review," *Reviews in Cardiovascular Medicine* 21 (2020): 205.

7. B. G. Winkel, A. G. Holst, J. Theilade, et al., "Nationwide Study of Sudden Cardiac Death in Persons Aged 1-35 Years," *European Heart Journal* 32 (2011): 983–990.

8. C. J. Hansen, J. Svane, P. E. Warming, et al., "Declining Trend of Sudden Cardiac Death in Younger Individuals: A 20-Year Nationwide Study," *Circulation* 151 (2024): 537–547.

9. T. J. Bowker, D. A. Wood, M. J. Davies, et al., "Sudden, Unexpected Cardiac or Unexplained Death in England: A National Survey," *QJM: An International Journal of Medicine* 96 (2003): 269–279.

10. D. Corrado, C. Basso, and G. Thiene, "Sudden Cardiac Death in Young People With Apparently Normal Heart," *Cardiovascular Research* 50 (2001): 399–408.

11. C. Glinge, R. Jabbari, B. Risgaard, et al., "Symptoms Before Sudden Arrhythmic Death Syndrome: A Nationwide Study Among the Young in Denmark," *Journal of Cardiovascular Electrophysiology* 26 (2015): 761–767.

12. M. N. Sheppard, J. Westaby, E. Zullo, B. V. E. Fernandez, S. Cox, and A. Cox, "Sudden Arrhythmic Death and Cardiomyopathy Are Important Causes of Sudden Cardiac Death in the UK: Results From a National Coronial Autopsy Database," *Histopathology* 82 (2023): 1056–1066.

13. G. Finocchiaro, D. Radaelli, D. Johnson, et al., "Yield of Molecular Autopsy in Sudden Cardiac Death in Athletes: Data From a Large Registry in the UK," *Europace* 26 (2024): euae029.

14. S. G. Priori, A. A. Wilde, M. Horie, et al., "HRS/EHRA/APHRS Expert Consensus Statement on the Diagnosis and Management of Patients With Inherited Primary Arrhythmia Syndromes," *Heart Rhythm* 10 (2013): 1932–1963.

15. E. Behr, D. A. Wood, M. Wright, et al., "Cardiological Assessment of First-Degree Relatives in Sudden Arrhythmic Death Syndrome," *Lancet* 362 (2003): 1457–1459.

16. J. C. Isbister, N. Nowak, L. Yeates, et al., "Concealed Cardiomyopathy in Autopsy-Inconclusive Cases of Sudden Cardiac Death and Implications for Families," *Journal of the American College of Cardiology* 80 (2022): 2057–2068.

17. J. C. Isbister, R. Tadros, H. Raju, and C. Semsarian, "Concealed Cardiomyopathy as an Emerging Cause of Sudden Cardiac Arrest and Sudden Cardiac Death," *Nature Cardiovascular Research* 3 (2024): 3.

18. C. Miles, A. Asimaki, I. C. Ster, et al., "Biventricular Myocardial Fibrosis and Sudden Death in Patients With Brugada Syndrome," *Journal of the American College of Cardiology* 78 (2021): 1511–1521.

19. A. D. Krahn, E. R. Behr, R. Hamilton, V. Probst, Z. Laksman, and H. C. Han, "Brugada Syndrome," *JACC. Clinical Electrophysiology* 8 (2022): 386–405.

20. M. N. Sheppard, *Practical Cardiovascular Pathology. Practical Cardiovascular Pathology*, 3rd ed. (CRC Press, 2022).

21. M. N. Sheppard, A. C. van der Wal, J. Banner, et al., "Genetically Determined Cardiomyopathies at Autopsy: The Pivotal Role of the Pathologist in Establishing the Diagnosis and Guiding Family Screening," *Virchows Archiv* 482 (2023): 653–669.

22. M. Papadakis, H. Raju, E. R. Behr, et al., "Sudden Cardiac Death With Autopsy Findings of Uncertain Significance: Potential for Erroneous Interpretation," *Circulation. Arrhythmia and Electrophysiology* 6 (2013): 588–596.

23. H. Quan, B. Li, C. M. Couris, K. Fushimi, P. Graham, and P. Hider, "Practice of Epidemiology Updating and Validating the Charlson Comorbidity Index and Score for Risk Adjustment in Hospital Discharge Abstracts Using Data From 6 Countries," (2011).

24. G. Mellor, H. Raju, S. V. de Noronha, et al., "Clinical Characteristics and Circumstances of Death in the Sudden Arrhythmic Death Syndrome," *Circulation. Arrhythmia and Electrophysiology* 7 (2014): 1078–1083.

25. S. L. Christiansen, C. L. Hertz, L. Ferrero-Miliani, et al., "Genetic Investigation of 100 Heart Genes in Sudden Unexplained Death Victims in a Forensic Setting," *European Journal of Human Genetics* 24 (2016): 1797–1802.

26. C. L. Hertz, S. L. Christiansen, L. Ferrero-Miliani, et al., "Next-Generation Sequencing of 100 Candidate Genes in Young Victims of Suspected Sudden Cardiac Death With Structural Abnormalities of the Heart," *International Journal of Legal Medicine* 130 (2016): 91–102.

27. J. D. Andersen, S. B. Jacobsen, L. C. Trudsø, M.-L. Kampmann, J. Banner, and N. Morling, "Whole Genome and Transcriptome Sequencing of Post-Mortem Cardiac Tissues From Sudden Cardiac Death Victims Identifies a Gene Regulatory Variant in NEXN," *International Journal of Legal Medicine* 133 (2019): 1699–1709.

28. D. T. Miller, K. Lee, N. S. Abul-Husn, et al., "ACMG SF v3.2 List for Reporting of Secondary Findings in Clinical Exome and Genome Sequencing: A Policy Statement of the American College of Medical Genetics and Genomics (ACMG)," *Genetics in Medicine* 25 (2023): 100866.

29. A. M. Roberts, J. S. Ware, D. S. Herman, et al., "Integrated Allelic, Transcriptional, and Phenomic Dissection of the Cardiac Effects of Titin Truncations in Health and Disease," *Science Translational Medicine* 7 (2015): 270ra6.

30. S. Richards, N. Aziz, S. Bale, et al., "Standards and Guidelines for the Interpretation of Sequence Variants: A Joint Consensus

Recommendation of the American College of Medical Genetics and Genomics and the Association for Molecular Pathology," *Genetics in Medicine* 17 (2015): 405–424.

31. P. H. Holm, K. B. Olsen, R. D. Maxime De Mets, and J. Banner, "Quantifying Cardiac Tissue Composition Using QuPath and Cellpose: An Accessible Approach to Postmortem Diagnosis," *Laboratory Investigation* 105 (2025): 102181.

32. S. Graham, Q. D. Vu, S. E. A. Raza, et al., "Hover-Net: Simultaneous Segmentation and Classification of Nuclei in Multi-Tissue Histology Images," *Medical Image Analysis* 58 (2019): 101563.

33. J. Gamper, N. A. Koohbanani, K. Benes, S. Graham, M. Jahanifar, and S. A. Khurram, "PanNuke Dataset Extension, Insights and Baselines," (2020).

34. K. He, X. Zhang, S. Ren, and J. Sun, "Deep Residual Learning for Image Recognition," (2015).

35. "Gray Level Co-Occurence Matrices (GLCM) Texture Features," accessed November 8, 2024, https://scikit-image.org/docs/stable/auto_examples/features_detection/plot_glcm.html.

36. "Scikit-Image Regionsprops," accessed November 8, 2024, https://scikit-image.org/docs/stable/api/skimage.measure.html#skimage.measure.regionprops.

37. M. Jon Henningsen, A. Khatam-Lashgari, K. Boisen Olsen, C. Jacobsen, C. Beltoft Brøchner, and J. Banner, "Translational Deep Phenotyping of Deaths Related to the COVID-19 Pandemic: Protocol for a Prospective Observational Autopsy Study," *BMJ Open* 11 (2021): 49083.

38. R Core Team, *R: A Language and Environment for Statistical Computing* (R Foundation for Statistical Computing, 2021).

39. Posit team, *RStudio: Integrated Development Environment for R* (Posit Software, PBC, 2023).

40. A. Liaw and M. Wiener, "Classification and Regression by randomForest," *R News* 2 (2002): 18–22.

41. N. Lunardon, G. Menardi, and N. Torelli, "ROSE: A Package for Binary Imbalanced Learning," (2014).

42. M. Kuhn, "Building Predictive Models in R Using the Caret Package," *Journal of Statistical Software* 28 (2008): 1–26.

43. J. Grau, I. Grosse, and J. Keilwagen, "PRROC: Computing and Visualizing Precision-Recall and Receiver Operating Characteristic Curves in R," *Bioinformatics* 31 (2015): 2595.

44. X. Robin, N. Turck, A. Hainard, et al., "pROC: An Open-Source Package for R and S+ to Analyze and Compare ROC Curves," *BMC Bioinformatics* 12 (2011): 1–8.

45. B. Schloerke, D. Cook, J. Larmarange, et al., *GGally: Extension to 'ggplot2'—GGally-Package* (GGally, 2024), accessed September 19, 2024, https://ggobi.github.io/ggally/reference/GGally-package.html.

46. H. Wickham, M. Averick, J. Bryan, et al., "Welcome to the Tidyverse," *Journal of Open Source Software* 4 (2019): 1686.

47. H. Wickham and J. Bryan, "readxl: Read Excel Files," accessed September 19, 2024, https://readxl.tidyverse.org/index.html.

48. D. Gohel and P. Skintzos, "flextable: Functions for Tabular Reporting," (2024).

49. D. D. Sjoberg, K. Whiting, M. Curry, J. A. Lavery, and J. Larmarange, "Reproducible Summary Tables With the Gtsummary Package," *R Journal* 13 (2021): 570.

50. S. De Jong, T. A. B. Van Veen, H. V. M. Van Rijen, and J. M. T. De Bakker, "Fibrosis and Cardiac Arrhythmias," *Journal of Cardiovascular Pharmacology* 57 (2011): 373–375.

51. T. P. Nguyen, Z. Qu, and J. N. Weiss, "Cardiac Fibrosis and Arrhythmogenesis: The Road to Repair Is Paved With Perils," *Journal of Molecular and Cellular Cardiology* 70 (2014): 83–91.

52. E. Sung, A. Prakosa, S. Zhou, et al., "Fat Infiltration in the Infarcted Heart as a Paradigm for Ventricular Arrhythmias," *Nature Cardiovascular Research* 1 (2022): 933–945.

53. L. Pakanen, H. Appel, A. Ahtikoski, et al., "Primary Myocardial Fibrosis — A Distinct Entity Characterized by Heterogeneous Histology," *Cardiovascular Pathology* 67 (2023): 107573.

54. C. Miles, B. J. Boukens, C. Scrocco, et al., "Subepicardial Cardiomyopathy: A Disease Underlying J-Wave Syndromes and Idiopathic Ventricular Fibrillation," *Circulation* 147 (2023): 1622–1633.

55. T. H. Lynge, C. M. Albert, C. Basso, et al., "Autopsy of All Young Sudden Death Cases Is Important to Increase Survival in Family Members Left Behind," *Europace* 26 (2024): 128.

56. D. K. Tansey, Z. Aly, and M. N. Sheppard, "Fat in the Right Ventricle of the Normal Heart," *Histopathology* 46 (2005): 98–104.

57. C. Basso and G. Thiene, "Adipositas Cordis, Fatty Infiltration of the Right Ventricle, and Arrhythmogenic Right Ventricular Cardiomyopathy. Just a Matter of Fat?," *Cardiovascular Pathology* 14 (2005): 37–41.

58. P. H. Holm, L. Hindsø, K. B. Olsen, and J. Banner, "Stereological Estimation of Myocardial Fat and Its Associations With Obesity, Epicardial, and Visceral Adipose Tissue," *Cells* 11 (2022): 11.

59. T. De Coster, P. Claus, I. V. Kazbanov, et al., "Arrhythmogenicity of Fibro-Fatty Infiltrations," *Scientific Reports* 8 (2018): 1–9.

60. R. Jayaraman, K. Reinier, S. Nair, et al., "Risk Factors of Sudden Cardiac Death in the Young: Multiple-Year Community-Wide Assessment," *Circulation* 137 (2018): 1561–1570.

61. M. Martini, M. Bueno Marinas, I. Rigato, K. Pilichou, and B. Bauce, "Clinical Insights in RNA-Binding Protein Motif 20 Cardiomyopathy: A Systematic Review," *Biomolecules* 14 (2024): 702.

62. A. D. den Haan, B. Y. Tan, M. N. Zikusoka, et al., "Comprehensive Desmosome Mutation Analysis in North Americans With Arrhythmogenic Right Ventricular Dysplasia/Cardiomyopathy," *Circulation. Cardiovascular Genetics* 2 (2009): 428–435.

63. A. A. M. Wilde and A. S. Amin, "Clinical Spectrum of SCN5A Mutations: Long QT Syndrome, Brugada Syndrome, and Cardiomyopathy," *JACC: Clinical Electrophysiology* 4 (2018): 569–579.

64. M. Vatta, E. Regalado, M. Parfenov, et al., "Analysis of TTN Truncating Variants in >74 000 Cases Reveals New Clinically Relevant Gene Regions," *Circulation: Genomic and Precision Medicine* 18 (2025): e004982.

65. D. S. Herman, L. Lam, M. R. G. Taylor, et al., "Truncations of Titin Causing Dilated Cardiomyopathy," *New England Journal of Medicine* 366 (2012): 619–628.

66. C. L. Grønholdt, B. L. Hansen, F. Folke, et al., "Diagnostic Yield in Families to Sudden Cardiac Death Victims: A 10-Year Follow-Up Study," *Europace* 27 (2025): 119.

67. A. Wisten, P. Krantz, and E. L. Stattin, "Sudden Cardiac Death Among the Young in Sweden From 2000 to 2010: An Autopsy-Based Study," *EP Europace* 19 (2017): 1327–1334.

68. E. D. Paratz, A. van Heusden, D. Zentner, et al., "Sudden Cardiac Death in People With Schizophrenia: Higher Risk, Poorer Resuscitation Profiles, and Differing Pathologies," *JACC. Clinical Electrophysiology* 9 (2023): 1310–1318.

69. J. Mujkanovic, P. E. Warming, L. V. Kessing, et al., "Nationwide Burden of Sudden Cardiac Death Among Patients With a Psychiatric Disorder Cardiac Risk Factors and Prevention," *Heart (British Cardiac Society)* 110 (2024): 1–7.

70. J. R. Busch and J. Banner, "Reliability of Police Reports When Assessing Health Information at the Forensic Post-Mortem Examination-Using Schizophrenia as a Model," *International Journal of Legal Medicine* 134 (2020): 1195–1201.

71. F. Domínguez, E. Adler, and P. García-Pavía, "Alcoholic Cardiomyopathy: An Update," *European Heart Journal* 45 (2024): 2294–2305.

72. A. Roset-Altadill, D. Wat, and M. Radike, "Cardiovascular and Pulmonary Complications of Recreational Drugs: A Pictorial Review," *European Journal of Radiology* 178 (2024): 111648.

73. D. Corrado, A. Anastasakis, C. Basso, et al., "Proposed Diagnostic Criteria for Arrhythmogenic Cardiomyopathy: European Task Force Consensus Report," *International Journal of Cardiology* 395 (2024): 131447.

74. P. D. Yazdanfard, A. H. Christensen, J. Tfelt-Hansen, H. Bundgaard, and B. G. Winkel, "Non-Diagnostic Autopsy Findings in Sudden Unexplained Death Victims," *BMC Cardiovascular Disorders* 20 (2020): 58.

75. J. Coelho-Lima, J. Westaby, and M. N. Sheppard, "Cardiac Arrest With Successful Cardiopulmonary Resuscitation and Survival Induce Histologic Changes That Correlate With Survival Time and Lead to Misdiagnosis in Sudden Arrhythmic Death Syndrome," *Resuscitation* 175 (2022): 6–12.

76. S. V. De Noronha, E. R. Behr, M. Papadakis, et al., "The Importance of Specialist Cardiac Histopathological Examination in the Investigation of Young Sudden Cardiac Deaths," *EP Europace* 16 (2014): 899–907.

Supporting Information

Additional supporting information can be found online in the Supporting Information section. **Data S1:** apm70169-sup-0001-DataS1.docx.